Formation & Dissociation of Methane Hydrates in Sediments.Part I : A New Experimental Set-up for Measurements and Modelling at the Core Scale

Olivier Bonnefoy, Jean-Michel Herri

▶ To cite this version:

HAL Id: hal-00126018

https://hal.archives-ouvertes.fr/hal-00126018

Submitted on 23 Jan 2007

Formation & Dissociation of Methane Hydrates in Sediments
Part I : A New Experimental Set-up for Measurements and Modelling at the Core Scale

Olivier Bonnefoy and Jean-Michel Herri *

Ecole Nationale Supérieure des Mines, Centre SPIN, URA CNRS n°2021, 158, Cours Fauriel, 42023 St.-Etienne, France

The ForDiMHyS project is a program devoted to experimental studies and the model development of the kinetics of FORmation and Dissociation of Methane Hydrates in Sediments. The first part of the project that is presented hereafter is designed to obtain experimental data on hydrate formation & dissociation under *in-situ* temperature and pressure conditions of methane hydrate in well constrained porous materials. The second part presented in another paper (Jeannin *et al.*, 2002) consists in modelling the flows inside the core; a specific numerical model has been developed to simulate the experimental set-up described in part one. The numerical model is 3D three phases and simulates the kinetics of hydrate dissociation and formation, taking into account the solubility of methane in water and the heat of phase transitions.

1 Introduction

More than 50% of the 18,8 Teratons (Kvenvolden, 1988) of organic carbon present on the earth is in form of gas hydrates located either in marine sediments or in the permafrost, *i.e.* in both cases in a porous medium. Hence the interest to study this crystalline compound in a porous medium and under controlled conditions to understand the formation processes that lead to such accumulations, to evaluate the feasibility of its industrial recovery as an energy resource and to quantify the mutual dependence of climate and amount of methane entrapped in natural porous media.

Since their discovery in laboratory by Sir Humphrey Davy (Davy, 1811), a lot of experimental results have been found on gas hydrates (Sloan, 1997) : 1) more than 130 compounds have been identified to form clathrate hydrates 2) three different crystalline structures have been discovered (Mak & MacMullan, 1965; Mac Mullan & Jeffrey, 1967; Ripmeester *et al.*, 1987) to represent the quasi-totality of them 3) stoechiometric ratio between water molecules forming cavities and guest molecule(s) has been observed to vary slightly around ideal values (Glew & Rath, 1966; Cady, 1983; Davidson & Ripmeester, 1984; …) phase diagrams have been established for a variety of single- or multi-components gas systems with or without thermodynamic inhibitor like alcohols or salts (Kobayashi, 1951; Katz *et al.*, 1959; Harmens & Sloan, 1990;…) 5) kinetics of hydrate nucleation from ice or water, growth and dissociation have been measured for different compounds, sometimes in presence of kinetic inhibitors (Englezos *et al.*, 1987; Skovborg & Rasmussen, 1994; Stern *et al.*, 1996; Herri *et al.*, 1999 and many others …) .

In parallel, modelisation has also continuously progressed : 1) theoretical models based on statistical thermodynamics have been successively developed to predict the equilibrium conditions of gas mixtures possibly in presence of inhibitors (Van der Waals & Platteuw, 1959; Parrish & Prausnitz, 1972; Chen & Guo, 1998; Klauda & Sandler, 2000) 2) conceptual models for nucleation and growth at the molecular level have been proposed (Barrer *et al.*, 1967; Vysniaukas & Bishnoi, 1983 Nzihou, 1994; Skovborg & Rasmussen, 1994, Herri, 1996) and 3) simulations carried out to go over the geological history of some natural sites.

More precisely, concerning porous media, we can distinguish two kinds of experimental works : the ones with a synthetic porous medium like silica gels, engraved plate or sand grains empilage (Handa & Stupin, 1992; Anderson *et al.*, 2001; Buffet & Zatsepina, 2000; …) and the others with a natural porous medium, which is typically a consolidated sediment sample (Booth *et al.*, 1999; …). A lot of results came out of these studies. However, no published results are available to show the dependence between the hydrate content of a porous medium and characteristics that are needed to constrain the different models used to simulate the formation and dissociation of methane hydrates in porous media. For this purpose, a new experimental set-up has been designed and constructed in the Ecole Nationale Supérieure des Mines de Saint-Etienne (France) with the financial help of industrial partners. In what follows, we will present the principle of the layout and then we will describe the whole apparatus and instrumentation which is inspired from the works of Stern *et al.*, 1998 and Booth *et al.*, 1999. A numerical simulation program has also been written to make profit of these results ; it is presented in the article of Jeannin *et al.*, 2002.

2.General Principle

It has been theoretically proven and experimentally observed that methane hydrate may form from dissolved methane and that this is the most

_____
* Corresponding author. E-mail: herri@emse.fr

promising track for explaining massive hydrate accumulation in marine sediments. Our equipment is primarily designed to reproduce in-situ conditions of this formation process *i.e.* the equipment allows to : 1) produce water containing a determined molar fraction of an hydrate-forming gas by saturating it in a mixer 2) let the saturated water continuously flow through a porous medium so that hydrate can form in its pores 3) inject the in-gas-impoverished water back in the saturator.

The installation is designed to work as a closed system (the gas phase pressure decreases when hydrate forms) or as an open isobaric system (during hydrate formation, fresh gas is injected to keep the gas phase pressure constant).
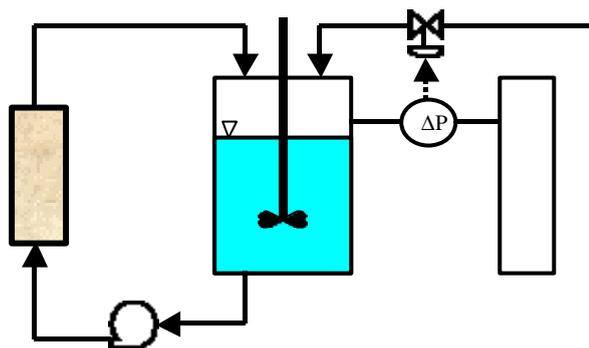

Figure 1 : Schematic of the installation

3. Material Specifications

Hereafter, we specify the technical characteristics of the vessels (saturator and reactor), of the active components (pump, gas flow rate controller and cryostats) and of the instrumentation (absolute and differential pressure transducers, gas flowmeter and temperature probes).

3.1 Vessels specifications

➤ Saturator (PARR Instruments) : this stainless steel vessel has a volume of 1,35 litres and is able to work under 350 bars. It is equipped with a double 6-blades propeller driven by a magnetic stirrer and has an external cooling jacket for temperature control. Three of the 4 holes for fittings are located at the top of the saturator *i.e.* in contact with the gas phase. On the fourth one, a plunger seal is screwed and allows the pump to suck up the water from the bottom of the saturator.

➤ Reactor (AUTOCLAVE Engineers) : this stainless steel vessel made to measure has a total volume of 9 litres and is designed to work under 280 bars. It comprises 2 tight chambers separated by a mobile piston. The upper chamber, or compression chamber, is filled with a refrigerant, agitated by a magnetic stirrer and cooled by a coil. The lower chamber, or confining chamber, contains a cylindrical porous medium sample wrapped in a flexible viton sleeve (85 sh) to isolate the pore fluid from the confining fluid, which pressure is at least 5 bars higher. The upper and lower chambers pressures are

independently adjustable so that any desired mechanical axial stress can be imposed on the porous medium. Among the 8 fittings of the reactor, 2 are dedicated to the process fluid and allow it to flow upwards through the sample before being re-injected in the saturator. The size of the sample is determined by the internal diameter of the reactor, which is of 15 cm and the maximum available height, which is of 25 cm. The sample may be either consolidated or a stack of distinct grains.

Figure 2 : Main reactor photograph

3.2 Active components specifications

➤ Pump (JASCO) : this HPLC analytical pump is able to work under 350 bars and may operate either in a constant flow rate mode or in a constant discharge pressure mode. The flow rate ranges between 1 µl/min to 10 ml/min and its accuracy is 2% of the setting in typical operating conditions (flowrate above 0,1 ml/min). A computer monitors this pump *via* an RS-232 interface.

➤ Gas flow rate controller : 1 electropneumatic valve (KÄMMER) is regulating the fresh gas injection when operating at isobaric conditions. The orifice size corresponds to a K_v of 4.10^{-5}.

➤ Cryostats (LAUDA) : The lower face of the reactor, its upper chamber and the saturator are independently refrigerated by 3 cryostats monitored by a computer *via* an RS-485 interface. The maximum flow rate is 17 litres/min and, depending on the cryostat, the minimum cooling temperature is –20°C or –35°C and the effective cooling capacity at 0°C is 0,15 or 0,22 kW.

➤ Gas booster : the pressurised gas supply is made directly with gas bottles (11 Nm³ each, gas purity of 99,95% or higher, 170 bars) or, when necessary to reach the installation design pressure of 280 bars with a gas booster commercialised by AUTOCLAVE Engineers.

3.3 Instrumentation specifications

➤ Pressure : 4 piezo-resistive pressure transducers (KELLER) measure the absolute pressures in the saturator, the compression chamber, the confining chamber and a reference chamber up to 300 bars and with a precision of 0,05% of the full scale. The 4-20 mA signal is displayed on a numerical indicator (WEST) and recorded on a computer *via* an RS-485 interface.

➤ Pressure difference : 3 capacitive pressure difference transducers (ROSEMOUNT) are installed. One of them measures the difference between the saturator pressure and the constant pressure of a reference chamber during isobaric formation so as to control the fresh gas injection and keep the saturator pressure stable. Its range is ±500 mbars. The two other transducers are directly connected to the lower and upper faces of the porous sample and measure the pressure drop. Their ranges are ±500 mbars and ±20 bars. The accuracy of these transducers is 0,05% of the full scale.

➤ Gas flowmeter : 1 mass-flowmeter (BROOKS) quantifies the fresh gas injection when operating at isobaric conditions. Based on thermal effect, the flowmeter can measure flow rates up to 200 Ncm^3/min *i.e.* $1,5.10^{-4}$ mole/s with an accuracy of 0,2% of the full scale plus 0,7% of the measure.

➤ Temperature : 8 platinum thermoresistances (PROSENSOR) measure the absolute temperatures in the saturator and at different points in the reactor. They comprise 3 wires and their accuracy is better than 0,1°C.

In addition, the main reactor is designed to receive three other sets of instruments.

➤ Mechanical properties : a load cell and a displacement gauge will be placed to determine the stress-strain relationship of the hydrated sample with time.
➤ Acoustic properties : one 1 MHz piezo-electric cell (PIE Ceramics) at each side of the core will be put to measure the compression ultrasonic waves speed and correlate it with the hydrate content. The emitting cell will be excited by a 300 volts pulse delivered in less than 1 ns by a generator (SOFRANEL) and the signal received by the other cell will be recorded on a PC-card (NATIONAL INSTRUMENTS) with a sampling frequency of 15 MHz.
➤ Electric properties : dedicated fittings are present on the lower cap of the reactor to allow electric resistivity measurements. Up to 16 electrodes may be placed around the porous sample so as to form a 3-dimensionnal map of the pores occupation rate.

The data acquisition is made by a commercial software (Labview, version 5.1) on a personal computer with a 16 Mo RAM and a 133 MHz Pentium micro-processor

3.4 Overall schematic
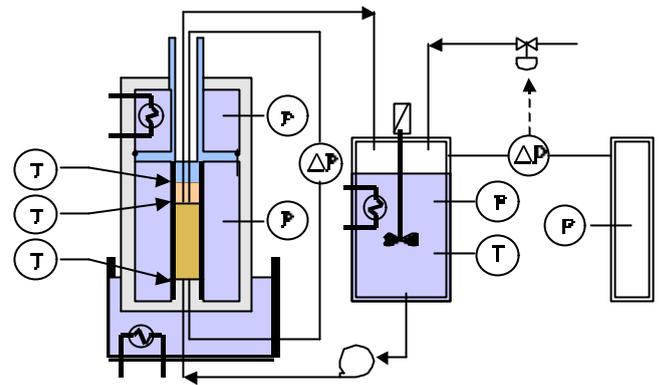The figure n°3 explains the general layout of the installation.

Figure 3 : Overall installation design

4. Simulated conditions

4.1 Pressure The design pressures of the different parts of the installation have been chosen to simulate the behaviour of a marine sediment sample under conditions given in figure n°4. The following values have been taken : 30% porosity ; 2700 kg/m^3 compacted sediment density ; 5 cm sample diameter.
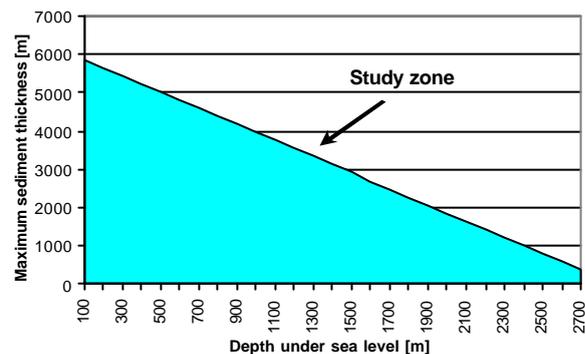

Figure 4 : Simulated pressure conditions

4.2 Permeability The combined measurements of the water flow rate and the pressure drop along the core sample in stationary state permits the determination of the hydraulic permeability with the help of a model like Kozeny-Carman's one.
For a typical sample of 10 cm length and 5 cm diameter, the permeability may be measured with a good accuracy (below 4%) between 0,1 mdarcys and 10 darcys which is a wide enough range to study oilrocks and sandstones .

4.3 Thermal conductivity As explained below in the experimental procedure, a cylindrical piece of PTFE is placed at the top of the porous medium sample and a temperature gradient is imposed along the core length. Basically, knowing the PTFE thermal conductivity and measuring the temperature difference between the top and the bottom of the PTFE piece, it is possible to estimate the axial heat flux through the porous medium. With this data and the measurement of the temperature difference between the bottom and the top of the core, it is possible to determine the thermal conductivity of the porous medium and correlate it with the hydrate content.

The accuracy of this method is of the order of 10% or less.

In effect, a complete numerical simulation of the heat equation with commercial software brought to the conclusion that radial heat losses may be safely neglected as shown in the figure n°5 where a temperature difference along the core is roughly 10°C.
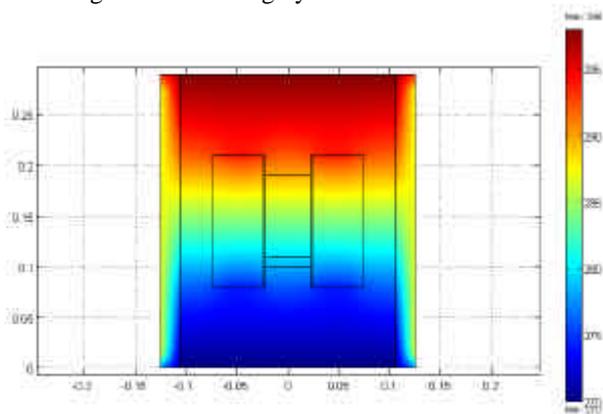

Figure 5 : Temperature profile of the sediment sample in the reactor

5. Operation protocol

The protocol is currently under construction but even if some modulations will be necessary, following steps are distinguished :

1. The core sample is placed vertically in the reactor with a PTFE piece of some centimetres thickness on its top and a 5 mm thick Viton sleeve around this assemblage. The two chambers of the reactor are then closed and filled with water.
2. The saturator temperature is set at about 35°C that is to say in a zone where gas solubility is very low whatever its pressure can be.
3. While the saturator pressure (*i.e.* the pore pressure) remains at atmospheric pressure, the confining pressure is raised to 20 to 40 bars and the pump turned on. The core sample is then flushed with distilled water to renew 100 times the pore volume and remove the trapped air bubbles.
4. Four 1-10 bars cycles are carried out to replace oxygen and nitrogen by hydrate-forming gas in the saturator before pressurising the latter. During the pressurisation, the pump is still functioning and a difference of 20 to 40 bars is always kept between confining pressure and pore pressure so the porous medium is correctly sealed off by the sleeve.
5. Once the final pressures are reached, the temperatures of the two reactor's chambers are adjusted to create a temperature gradient along the sample, the lowest temperature being at the bottom. These two temperatures are chosen so that the equilibrium temperature under the saturator pressure is roughly in the middle of the core.
6. After all temperatures and pressures are stabilised, the saturator temperature is decreased just above the equilibrium temperature at the saturator pressure. In the sort, the dissolved amount of hydrate-forming gas is maximum in the saturator but no hydrate can form but in the upper half of the sample.

During all these steps, the relative and differential pressures, the temperatures as well as the liquid flow rate are recorded on a computer. With a mass balance on dissolved methane in water, the amount of hydrate can be calculated and correlations established with thermal conductivity and hydraulic permeability.

6. Conclusion

To summarize, this new apparatus is designed to simulate pressure and temperature conditions met in marine sediments and permafrost where large quantities of methane are entrapped. The apparatus allows the migration of methane dissolved in water through natural consolidated porous samples and the study of its formation and dissociation kinetics. Also, it will provide experimental correlations between hydrate content and sediment characteristics like thermal conductivity, hydraulic permeability, compression waves velocity and electric resistivity. The experiments are currently underway and their results will lead to mathematical models validation.

Acknowledgment

References

Anderson R., Biderkab A.B., Tohidi B. & Ben Clennell M. (2001) Visual Observation of gas hydrate formation in glass micromodels, Proc. of 63rd EAGE Annual Conf., Amsterdam.

Barrer R.M., Edge F.R.S. & Edge A.V.J. (1967) Gas hydrates containing Argon, Krypton and Xenon – Kinetics and energetics formation and equilibria, Proc. Roy. Soc., A300, No. 08/22, p. 1-24

Booth J.S., Winters W.J. & Dillon W.P. (1999) Oct. 4, Apparatus investigates geological aspects of gas hydrates, Oil & Gas Journal – Special, p. 63-69

Buffett B.A. & Zatsepina O.Ye. (2000) Formation of Gas hydrate from dissolved gas in natural porous media, Marine Geology, 164, No 1-2, p.69-77

Cady G.H. (1983) J. Phys. Chem., 85, 4437

Chen G.-J. & Guo T.M. (1998) A new approach to Gas Hydrate modeling, Chem. Eng. J., 71, p.145-151

Davidson D.W. & Ripmeester J.A. (1984) Inclusion Compounds, Atwood J.L., Davies J.E.D. & MacNichol D.D. Eds., Academic Press, 3, Chapter 3

Davy H. (1811) Phil. Trans. Roy. Soc. London, 101, 1

Englezos P., Kalogerakis N., Dholabhai P.D. & Bishnoi P.R. (1987) Kinetics of Formation of Methane and Ethane gas Hydrates, Chem. Eng. Sci., 42, p.2647-2658

Glew D.N. & Rath N.S. (1966) J. Chem. Phys., 44, 1710

Handa Y.P. & Stupin D. (1992) Thermodynamic properties and Dissociation Characteristics of Methane and Propane Hydrates in 70-A-Radius Silica Gel Pores, J. Phys. Chem., 96, p.8599-8603

Harmens A. & Sloan E.D. (1990) Can. J. Chem. Eng., 68, 151

Herri J.-M. (1996) Etude de la formation de l'hydrate de méthane par turbidimétrie *in-situ*, PhD dissertation, Université Pierre et Marie Curie, Paris VI

Herri J.M., Gruy F., Pic J.-S., Cournil M., Cingotti B. & Sinquin A. (1999) Chem. Eng. Sci., $\underline{54}$, 1849

Jeannin L., Bayi A., Renard G., Bonnefoy O. & Herri J.M. (2002) Formation & Dissociation of methane hydrates in sediments – Part II : Numerical modelling, Proc. of the 4th ICGH, Yokohama, Japan

Jeffrey G.A. & McMullan R.K. (1967) Prog. Inorg. Chem., $\underline{8}$, 43

Katz D.L., Cornell D., Kobayashi R., Poettmann F.H.,

Klauda J.B. & Sandler S.I. (2000) A fugacity model for Gas hydrate Phase Equilibria, Ind. Eng. Chem. Res., $\underline{39}$, p.3377-3386

Kobayashi R. (1951) Vapor-Liquid Equilibrium in Binary Hydrocarbon-Water Systems, PhD Dissertation, U. Mich. University microfilms No.3521, Ann Arbor, MI

Kvenvolden K.A. (1988) Chem. Geol., $\underline{71}$, 41

Mak T.C.W. & McMullan R.K. (1965) J. Chem. Phys., $\underline{42}$, 2732

Parrish W.R. & Prausnitz J.M. (1972) Dissociation pressure of gas hydrates formed by gas mixtures, Ind. Eng.Chem. Process Des. Dev., $\underline{11}$, p. 26-35

Ripmeester J.A., Tse J.A., Ratcliff C.I. & Powell B.M. (1987) Nature, $\underline{325}$, 135

Skovborg P. & Rasmussen P. (1994) Chem. Eng. Sci., $\underline{49}$, 1131

Sloan E.D. (1997) Clathrate Hydrates of Natural Gases, 2nd edition, Marcel Dekker, New-York

Stern L.A., Kirby S.H. & Durham W.B. (1996) Science, $\underline{273}$ p.1843

Stern L.A., Kirby S.H. & Durham W.B. (1998) Polycristalline methane hydrate : synthesis from superheated Ice and low-temperature mechanical properties, Energy & Fuels, $\underline{12}$, No 2, p.201-211

Van Der Waals J.H. & Platteuw J.C. (1959) Clathrate solutions, Adv. Chem. Phys., $\underline{2}$, No 1, p. 1-57

Vary J.A., Elenbaas J.R. & Weinaug C.F. (1959) Handbook of Natural Gas Engineering, McGraw-Hill, New-York, p. 802

Vysniaukas A. & Bishnoi P.R. (1983) A kinetic study of Methane Hydrate Formation, Chem. Eng. Sci., $\underline{27}$, p. 1197-2103